Hindawi
Complexity
Volume 2019, Article ID 5491298, 11 pages
https://doi.org/10.1155/2019/5491298

*Research Article*

# Gait Regulation of a Bionic Quadruped Robot with Antiparallelogram Leg Based on CPG Oscillator

**Jiupeng Chen**,[1] **Hongjun San**,[1,2] **and Xing Wu**[1]

[1]*Faculty of Mechanical and Electrical Engineering, Kunming University of Science and Technology, Kunming, Yunnan, China*
[2]*Key Laboratory of Panax Notoginseng in Yunnan Province, Kunming, Yunnan, China*

Correspondence should be addressed to Hongjun San; sanhjun@163.com

Received 19 July 2019; Revised 13 October 2019; Accepted 6 November 2019; Published 30 November 2019

Academic Editor: Chittaranjan Hens



In order to shorten the research and development cycle of quadruped robot, it is significant to solve the problem of single leg weight-bearing and obtain a smooth gait switching. Firstly, a leg structure with an antiparallelogram is proposed, which greatly enhances the strength and stiffness of the leg in this paper. Secondly, the Simulink-ADAMS cosimulation platform is built and the improved Hopf oscillator is used in the control of robot. This control mode based on CPG realizes the walk and trot gait of quadruped robot. Thirdly, in order to solve the problems of breakpoints, phase-locked, and stopping of gait curve in the process of gait switching by directly replacing the gait matrix, the functional relationship between the right hind leg and duty cycle is introduced to realize the smooth transition of gait curve. The simulation results show that the proposed algorithm can achieve a smooth gait transformation within 4–6 second, which preliminarily proves the feasibility of the algorithm. Finally, the experimental platform is built and the control algorithm is written into the controller to realize the specific gait of the robot, which proves the effectiveness of the proposed method.

## 1. Introduction

Because of the scattered landing points, the foot robot can flexibly adjust its walking posture in the foot reachable area and reasonably select the support points, so it has higher ability of obstacle avoidance and obstacle surmounting. It has good application prospects in rescue and disaster relief, mine clearance, geographic exploration, and so on. It is one of the hotspots in the field of robotics research [1–3]. Seral legs are the most mature leg structure studied at present, which is widely used in quadruped robots, such as Big-Dog, Little-Dog, and Cheetah developed by Boston Dynamics Company, USA [4, 5], and hydraulic-driven quadruped bionic robot developed by Shandong University [6]; this structure has the characteristics of easy control and simple structure, but its strength and stiffness are low. Parallel leg mechanism has become a better choice for walking robot than series leg mechanism because of its high load-carrying capacity and stability; however, this leg type control is complex and difficult to realize industrialization [7–10]. For example, the robot designed by Para-walker of Tokyo University of Technology, the four reconfigurable walker proposed by Wang et al. of Yanshan university [8] and the new walking robot based on 3-RPC parallel mechanism proposed by Zhang and Li. We can see from the above that both series legs and parallel legs have their limitations in application. It is an urgent problem to study the leg configuration of a quadruped robot with convenient control and simple structure.

On the basis of structural design, the control of quadruped robots is also a complex and arduous task. CPG (central pattern generator) is located in the spinal cord of animals and produces rhythmic signals with stable phase interlocking relationship [11]. Biological CPG consists of several central neurons, which are composed of three basic neurons: excitation, lateral inhibition, and terminal cross inhibition [12, 13]. Through synaptic connections, each neuron exhibits a variety of output behaviors, controlling animals to achieve a variety of motor patterns [14]. At present, the typical CPG models used in robot motion

control can be divided into two categories: the model based on the central neuron and the model based on the nonlinear oscillator [15]. Based on the model of the central neuron (e.g., Matsuoka model and Kimura model), its physical meaning is clear, but there are many regulating parameters [16, 17]. The model based on the nonlinear oscillator (e.g., Hopf model and van der Pol model) has fewer adjusting parameters and strong practicability [18, 19]. The CPG can interact with the upper neural network and lower neural network and can realize the walking of the quadruped robot on irregular ground. At the same time, adjusting the parameters of the CPG model can change the gait characteristics of the robot [20, 21].

Santos and Matos established a CPG model based on the Hopf oscillator, adjusted the parameters of the Hopf oscillator, and verified the effectiveness of this method on AIBO machine dog [22]. According to the structural characteristics of quadruped robots, Xu et al. built a fully symmetric CPG network model based on the Hopf oscillator model [23]. Wang et al. constructed a new model of the bionerve central mode generator unit by using the universal Hopf oscillator as neuron, which solved the problem that the joint driving oscillation signal of the existing joint-like bionic robot could not be controlled [24]. Wang studied the gait planning of a quadruped robot, modeled and analyzed the bionic structure, and studied the robot based on the foot-end trajectory planning and CPG gait generation strategy [25]. Zhao studied a quadruped robot and realized its static walking and diagonal walking by using MATLAB and ADAMS simulation [26].

All the above studies are based on CPG modeling of series legs, which makes the whole mechanism lack the necessary strength and stiffness. Whether the CPG oscillation of the improved leg configuration is practical or not is an urgent problem to be solved. Therefore, a quadruped bionic robot named MQ robot is proposed in this paper. The antiparallelogram mechanism is used in the legs of the robot, which greatly improves the strength and stiffness of the legs. At the same time, in order to solve the problem of the sudden change of speed and acceleration caused by the direct replacement of the gait matrix, the Hopf oscillator is used to realize the smooth transition of gait switching. The innovations of this paper are as follows: (i) a new antiparallelogram leg configuration is proposed; (ii) for the first time, a Hopf oscillator is applied to the antiparallelogram leg structure and realized control; and (iii) in the process of gait switching, transfer function is introduced to realize the stability of the gait switching process.

## 2. Brief Description of Mechanism

The robot presented in this paper consists of forepart, hindside, waist structure, lateral pendulum, and leg structure. The robot is controlled by 12 motors and can achieve two gaits: static walk and diagonal trot. In order to get closer to the real animal motion, the leg configuration here uses knee-to-elbow configuration, which can improve the stability of the robot. Figure 1 shows the structure of the MQ quadruped robot. In order to make the motion mode of the robot close

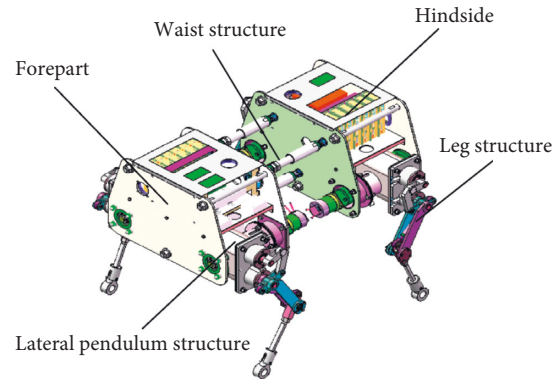


Figure 1: The 3D model of the MQ quadruped robot.

to that of mammals, a three-degree-of-freedom parallel mechanism is used as the waist of the quadruped robot, which enables the robot's forepart to have pitching motion, left-right rotation, and forward-backward telescopic motion relative to its hind-side. The robot is driven by a DC servo motor, and its power source is a portable lithium battery.

In order to make up for the shortcomings of low strength and stiffness and poor load capacity of series leg mechanism, the leg configuration with antiparallelogram mechanism is designed in this paper as shown in Figure 2. Two motors mounted on the leg realize the output motion of the foot end. The leg has two parallelograms, which greatly improves the strength and stiffness of the quadruped robot.

## 3. CPG Model and Network Structure of Quadruped Robot

Because the Hopf oscillator will form a stable limit cycle in space, which can move from any state to stable operation and can produce stable periodic oscillation signal. Secondly, the Hopf oscillator is a simple harmonic oscillator, whose output signal amplitude and frequency are easy to control. Therefore, this paper uses the Hopf oscillator to establish the joint output curve. Its mathematical model is shown in

$$\begin{cases} \dot{x} = \alpha(u - r^2)x - \omega y, \\ \dot{y} = \alpha(u - r^2)x - \omega x, \end{cases} \tag{1}$$

where $x$ and $y$ are state variables, $u$ determines the amplitude of the oscillator and $A = \sqrt{u}$, $\omega$ is the frequency of the oscillator, and $\alpha$ is used to control the oscillator's convergence rate to the limit cycle.

Figure 3 shows the stability limit cycle formed by the Hopf oscillator in space, so it can be controlled by the Hopf oscillator at the joint of the robot to improve the stability of quadruped walking. Under different road conditions, the two output curves of the same oscillator can realize direct foot coupling between the hip joint and knee joint, so that the limit cycle does not diverge and achieves a self-stabilizing effect.

Figure 4 shows the output curve of the oscillator, the blue curve can be used as a driving curve of the hip joint, and the red curve can be used as driving curve of the knee joint. These curves indicate that the rising part of $x$ curve

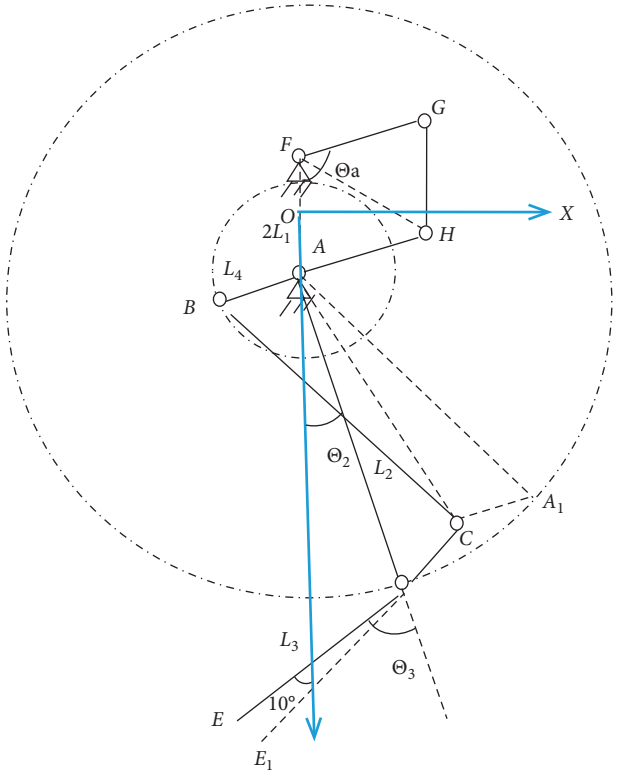


Figure 2: Leg mechanism analysis.

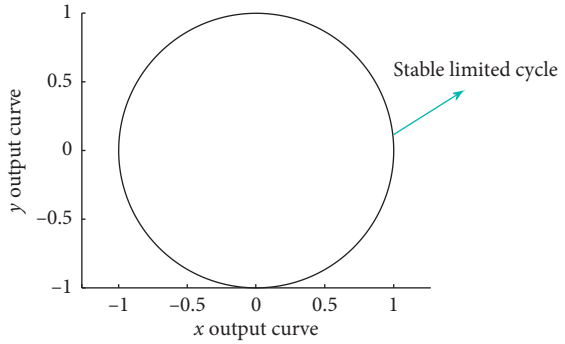


Figure 3: Limit cycles of stability.

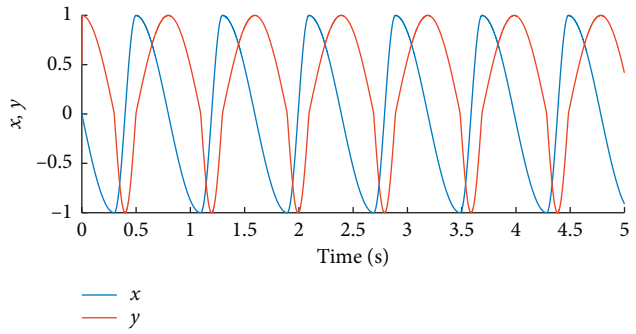


Figure 4: Hopf oscillator output.

corresponds to curve $y$ less than zero, and the falling part of $x$ corresponds to $y$ greater than zero.

Therefore, the output of the oscillator can be used as the control signal for robot joint. In previous studies, only one curve of oscillator can be used effectively, which results in low utilization rate and high control complexity of oscillator. In this way, an oscillator can control both joints of a single leg at the same time, and this process can reduce the number of oscillators used. In order to make the robot adapt to different road conditions, it is necessary to adjust its gait to get the best motion state.

The improvement of the Hopf oscillator can be obtained as follows:

$$\begin{cases} \begin{bmatrix} \dot{x}_i \\ \dot{y}_i \end{bmatrix} = \begin{bmatrix} \alpha\left(u - r_i^2\right) & -\omega_i \\ \omega_i & \alpha\left(u - r_i^2\right) \end{bmatrix} \begin{bmatrix} x_i \\ y_i \end{bmatrix} \\ \quad + \sum_{j=1}^{4} R\left(\theta_i^j\right) \begin{bmatrix} x_i \\ y_i \end{bmatrix}, \qquad i = 1, \ldots, 4, \\ r_i^2 = x_i^2 + y_i^2, \\ \omega_i = \dfrac{\omega_{st}}{e^{-ay_i} + 1} + \dfrac{\omega_{sw}}{e^{ay_i} + 1}, \\ \omega_{st} = \dfrac{1 - \beta}{\beta} \omega_{st}, \\ \theta_{hi} = x_i, \\ \theta_{ki} = \begin{cases} -\operatorname{sgn}(\varphi) \dfrac{A_k}{A_h} y_i, & y_i \le 0, \\ 0, & y_i > 0, \end{cases} \end{cases} \tag{2}$$

where $\beta$ is duty cycle; $\omega_{sw}$ is the swing phase frequency; $\omega_{st}$ is the supporting phase frequency; $\theta_{hi}$ is the hip control curve; $\theta_{ki}$ is the knee control curve; $a$ is a normal number, which determines the transformation speed of the swing phase and the supporting phase; $A_h$ is the hip swing amplitude; and $A_k$ is the knee swing amplitude.

$R(\theta_i^j)$ represents a gait matrix, which describes the coupling relationship between oscillators, and its expression is as follows:

$$R\left(\theta_i^j\right) = \begin{bmatrix} \cos\theta_{ji} & -\sin\theta_{ji} \\ \sin\theta_{ji} & \cos\theta_{ji} \end{bmatrix}, \tag{3}$$

where $\theta_i^j = \theta_{ji} = 2\pi(\varphi_i - \varphi_j)$, $\varphi_i$ is the phase of the $i$th oscillator.

For gait research of robots, there is no need to use the degree of freedom of lateral swing, so eight Hopf oscillators

are needed to control the eight rotating joints of the robot's legs. For equation (2), the motion curves of the hip and knee joints of one leg can be obtained. For the improved Hopf oscillator, one oscillator can produce two outputs, so only four Hopf oscillators are needed for the four legs of the robot to construct the CPG control network.

For ease of description, the left foreleg is represented by LF, the right foreleg by RF, the left hind leg by LH, and the right hind leg by RH, as shown in Figure 5. In most cases, quadruped robots have different gaits, such as static walking and diagonal trotting. Because the walking mode will affect the dynamic performance of the robot, it is very important to select the appropriate CPG parameters in different environments and then adjust the control output curve. The network topology diagram shown in Figure 5 indicates the coupling relationship of the quadruped robot oscillator. Fine tuning the parameters of the oscillator can achieve the stability of the robot in various situations and ensure that the output curve meets the expected control objectives.

## 4. Walk Gait Simulation Analysis

Cosimulation platform combines the advantages of control software and dynamics software and is widely used in robot control. As a multibody dynamics software, ADAMS has powerful modeling and analysis functions. It is the most widely used analysis software in the world. However, its control function is weak, and it often needs external interface to realize its control function. Simulink has powerful control function and can use graphical module to realize complex control. However, its modeling ability is not enough to analyze complex objects.

In order to use the output curve of the Hopf oscillator to drive the quadruped robot, the control system is built in Simulink, the mechanical dynamics system is built in ADAMS, and the interface relationship between ADAMS and Simulink is established. The dynamic simulation platform of the quadruped robot is shown in Figure 6, and the ADAMS multibody dynamics system is shown in Figure 7.

Static walking is the most commonly used walking mode in quadruped mammals. Each leg runs alternately to achieve a stable gait. Although the running speed of this gait is low, its stability is high and it can meet the requirements of long-term walking.

Set the CPG model parameters to $\alpha = 10000$, $u = 1$, $a = 100$, $\omega_{sw} = 5\pi$, $\beta = 0.75$, and $\varphi_{RH} = 0.25$. From Figures 8 and 9 we can see that the output curve of the oscillator strictly conforms to the motion law of the robot joint. Figure 8 shows the four legs of the robot moving in turn, with a phase difference of 0.25. Figure 9 shows that the motion curves of the hip and knee joints during gait switching strictly conform to the motion laws of the elbow joints.

## 5. Trot Gait Simulation Analysis

Diagonal trotting gait is the most ideal gait in dynamic walking. Its diagonal leg has the same phase and can be regarded as a virtual leg. This virtual leg alternately moves with another diagonal virtual leg to complete the dynamic walking of the robot. Compared with other dynamic gaits, this gait has higher stability and better dynamic characteristics.

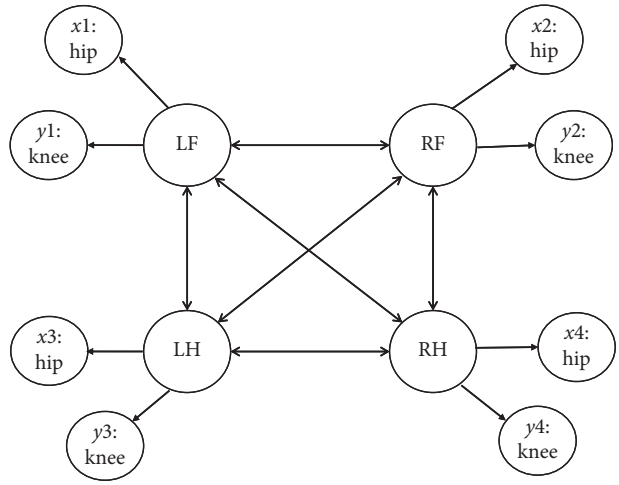


Figure 5: Topological structure of the CPG oscillator network.

Set the CPG model parameters to $\alpha = 10000$, $u = 1$, $a = 100$, $\omega_{sw} = 5\pi$, $\beta = 0.5$, and $\varphi_{RH} = 0$. From Figures 10 and 11, it can be seen that the output curve of the oscillator strictly conforms to the motion law of the robot joint. Figure 10 shows that the robot's diagonal legs are lifted and landed simultaneously with a phase difference of 0.5. Figure 11 shows that the motion curves of the hip and knee joints during gait switching strictly conform to the motion laws of the elbow joints.

## 6. Walk-Trot Gait Transform

In previous studies, changing the phase relationship between CPG oscillating units can control the quadruped robot to switch from the current motion mode to other motion modes. At present, the commonly used gait conversion methods are changing the network characteristics of the CPG [12, 27], changing the external excitation signal [28, 29], changing the characteristics of the nerve oscillator itself [30], and adding instantaneous interference [31].

This paper achieves gait switching by changing the characteristics of the CPG network. In most cases, this direct replacement of the gait matrix to achieve gait switching will cause unexpected results. Figure 12 shows that in 4–6 seconds, when the walk gait is switched to the trot gait, breakpoints, phase-locked, and stopping phenomena will occur, which will lead to sudden changes in speed and acceleration during the robot's movement and easily lead to the robot losing its stability. Figure 13 shows that the motion curve of the hip and the knee joint during gait switching strictly conforms to the motion law of the elbow joint.

In the process of gait switching, if we cannot solve these problems of breakpoints, phase-locked, and stopping phenomena, the system power will be consumed and the stability will be lost. Gait switching is to adapt to the basic links

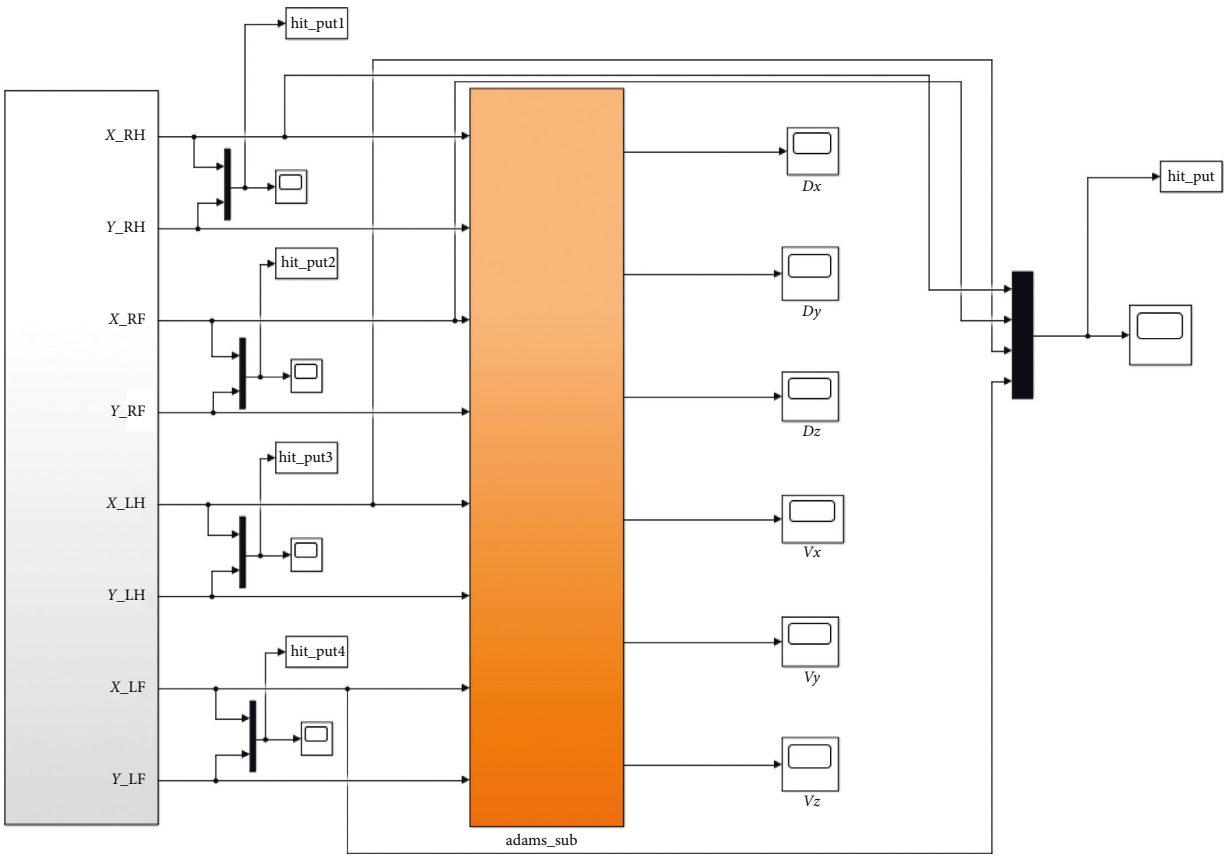


Figure 6: ADAMS & Simulink cosimulation platform.

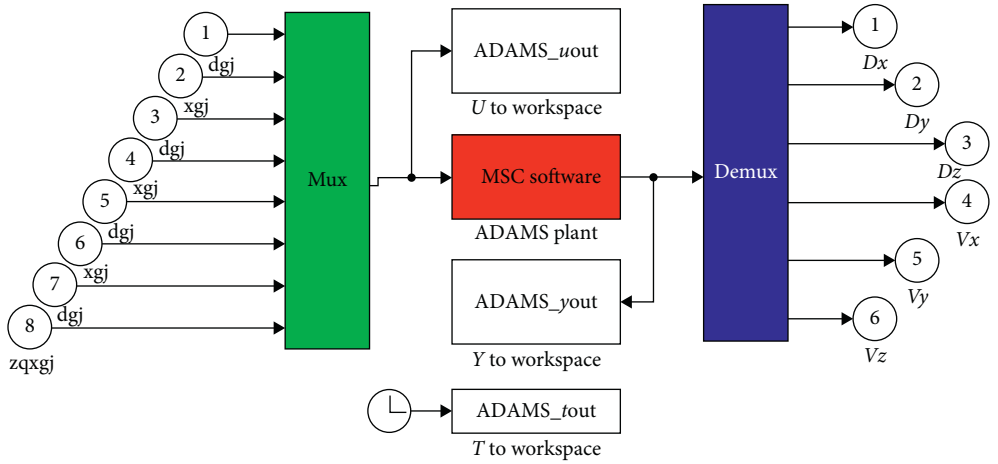


Figure 7: ADAMS multibody dynamics system.

of different roads, so it is a very urgent task, which is also the focus of this paper.

In this paper, the walk and trot gait of the robot are studied in order to verify the correctness of the proposed robot motion mode. We can make the robot switch between different gaits by changing the gait matrix, Figures 14 and 15 show the relative phase relationship between the walk and trot gait.

In order to improve the stability of the robot and ensure the smoothness of the gait switching curve, it is necessary to solve the problem that the gait curve is not smooth and the swing amplitude is large through the algorithm. From the observation of Figures 14 and 15, it can be seen that the phases of the left foreleg (LF) and the right foreleg (RF) of the quadruped robot remain unchanged during the transition from the walk gait to the trot gait:

$$\begin{aligned} \varphi_1 &= 0, \\ \varphi_2 &= 0.5. \end{aligned} \tag{4}$$

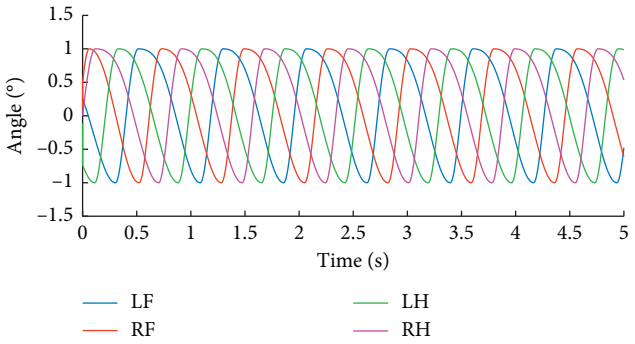


Figure 8: Phase relationship of the hip joint in the walk gait.

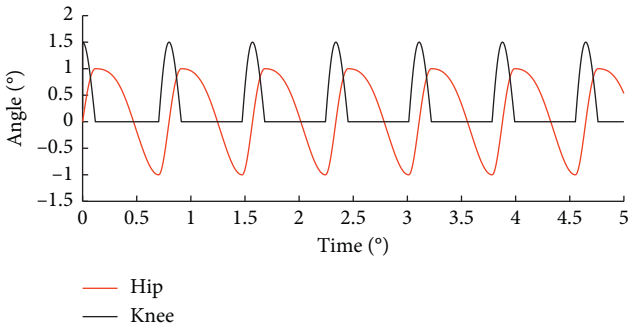


Figure 9: The relationship between the hip and the knee rotation angle in the walk gait.

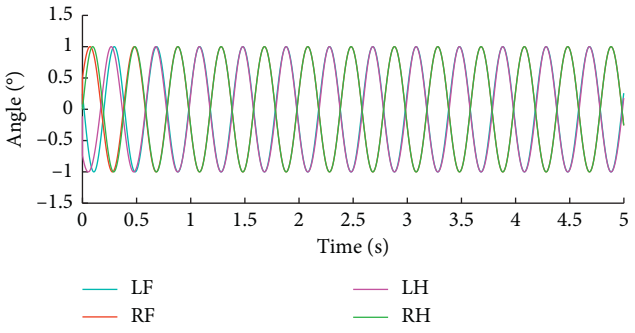


Figure 10: Phase relationship of the hip joint in the trot gait.

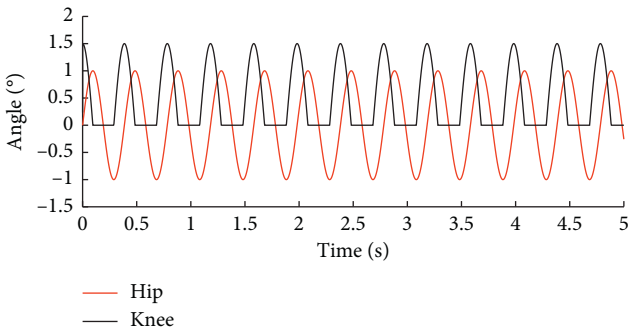


Figure 11: The relationship between the hip and the knee rotation angle in the trot gait.

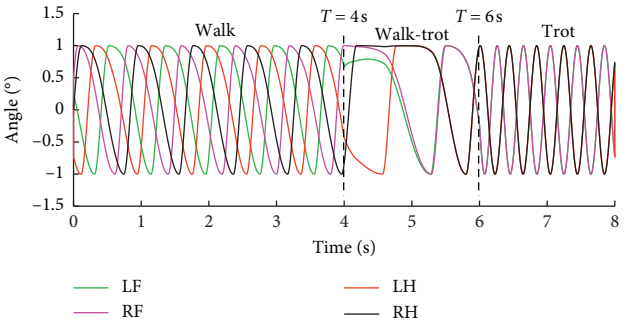


Figure 12: Gait conversion by replacing the gait matrix.

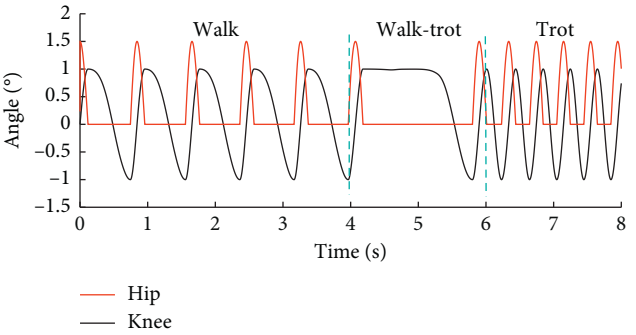


Figure 13: Control curve of the hip and the knee joint of LF.

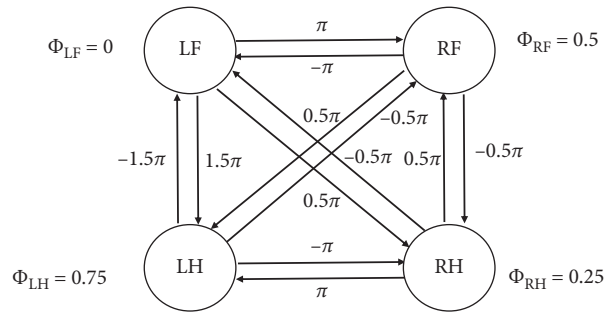


Figure 14: Relative phase relation of the walk gait.

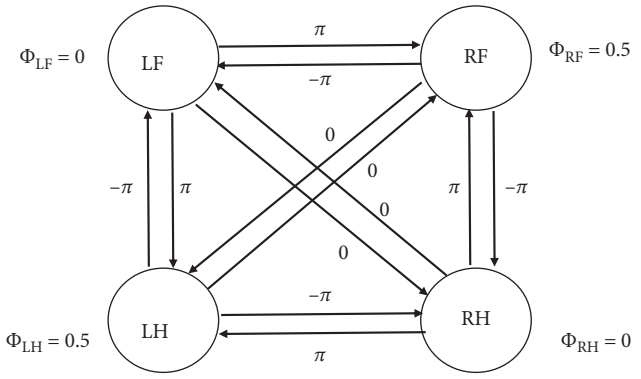


Figure 15: Relative phase relation of the trot gait.

The left hind leg phase $\varphi_4$ and duty cycle $\beta$ of a quadruped robot can be expressed by the right hind leg phase $\varphi$. According to the relationship between the two gait phases, it can be concluded that

$$\begin{aligned} \varphi_4 &= 0.5 + \varphi, \\ \beta &= 0.5 + \varphi. \end{aligned} \tag{5}$$

Therefore, the right hind leg phase $\varphi$ can be set to change from 0.25 to 0, which can realize the switch from the walk gait to trot gait, as shown in the following equation:

$$\varphi = \begin{cases} 0.25, & 0 < t < 4, \\ \dfrac{-t}{8} + \dfrac{3}{4}, & 4 \le t \le 6, \\ 0, & t > 6, \end{cases} \tag{6}$$

$$\begin{cases} \theta_{11} = 0, \\ \theta_{21} = -\pi, \\ \theta_{31} = -\varphi \cdot 2\pi, \\ \theta_{41} = -(0.5 + \varphi) \cdot 2\pi, \end{cases} \tag{7}$$

$$\begin{cases} \theta_{12} = \pi, \\ \theta_{22} = 0, \\ \theta_{32} = (0.5 - \varphi) \cdot 2\pi, \\ \theta_{42} = -\varphi \cdot 2\pi, \end{cases}$$

$$\begin{cases} \theta_{13} = \varphi \cdot 2\pi, \\ \theta_{23} = (\varphi - 0.5) \cdot 2\pi, \\ \theta_{33} = 0, \\ \theta_{43} = -\pi, \end{cases} \tag{8}$$

$$\begin{cases} \theta_{14} = (\varphi + 0.5) \cdot 2\pi, \\ \theta_{24} = \varphi \cdot 2\pi, \\ \theta_{43} = -\pi, \\ \theta_{44} = 0. \end{cases}$$

It can be seen from Figure 16 that the curve of walk gait switching to trot gait is smooth and stable, and there are no breakpoints, phase-locked, and stopping phenomena, which proves the effectiveness of the proposed algorithm.

Figure 17 is the driving curve of the left foreleg (LF), which conforms to the motion law of the hip and knee of the oscillator. The smooth transition of the quadruped robot is achieved during the motion process, which proves the effectiveness of the proposed method.

Figure 18 shows the results of Simulink-ADAMS cosimulation at different times. Yellow means that the robot's feet are off the ground. When $t \le 4$ s, the robot runs steadily according to the static gait of 1-4-2-3 phase sequence. When $4\text{ s} < t < 6$ s, the gait switching occurs. When $t \ge 6$ s, the robot is in a diagonal trot gait. It can be seen that the robot walks along the output curve of the oscillator and successfully realizes the gait switching.

Although the smooth gait switching can be achieved by reasonable processing of the Hopf oscillator and introducing

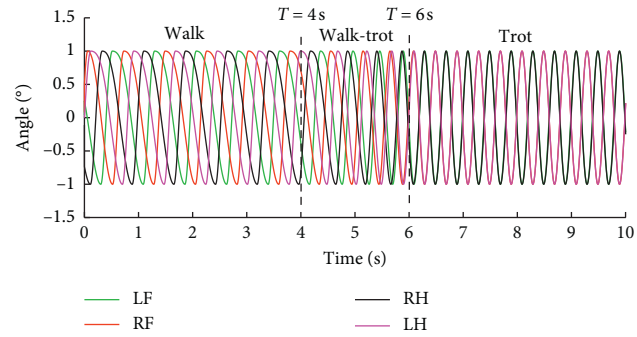


Figure 16: Phase relationship of the hip joint in gait switching for walk-trot.

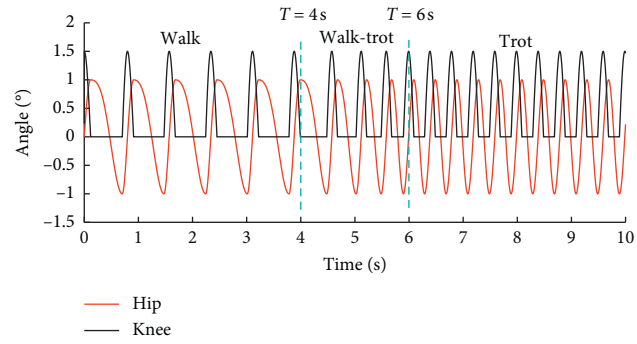


Figure 17: The relationship between hip and knee rotation angles.

transfer function, it is necessary to determine whether the quadruped robot can maintain stable operation during the switching process. In order to describe the stability of gait, the displacement and velocity curves of the robot in the course of walking are given in Figure 19. The displacement curve is on the left and the velocity curve is on the right. From the displacement curve, it can be seen that the lateral fluctuation of the robot is very small and the maximum fluctuation rate is 1.244%, which shows that the robot can basically keep straight walking. At the same time, the center of mass of the robot fluctuates within a reasonable range, and the maximum fluctuation rate is 0.682%, which indicates that the robot can walk steadily. From the velocity curve on the right side, it can be seen that the curve conforms to the laws of static gait and diagonal gait and has periodic fluctuation. The forward displacement can transition smoothly during the switching period, and the diagonal trot gait after switching has a larger slope than the static gait, which conforms to the biological movement law.

## 7. Construction of the Experimental Platform

The gait switching experiment is complex and difficult in the actual operation process. This requires not only good motor tracking performance, but also improved controller performance. The controller acts as the master station and 8 drivers act as the slave station. The transmission of signals between master station and slave station can be greatly improved by using

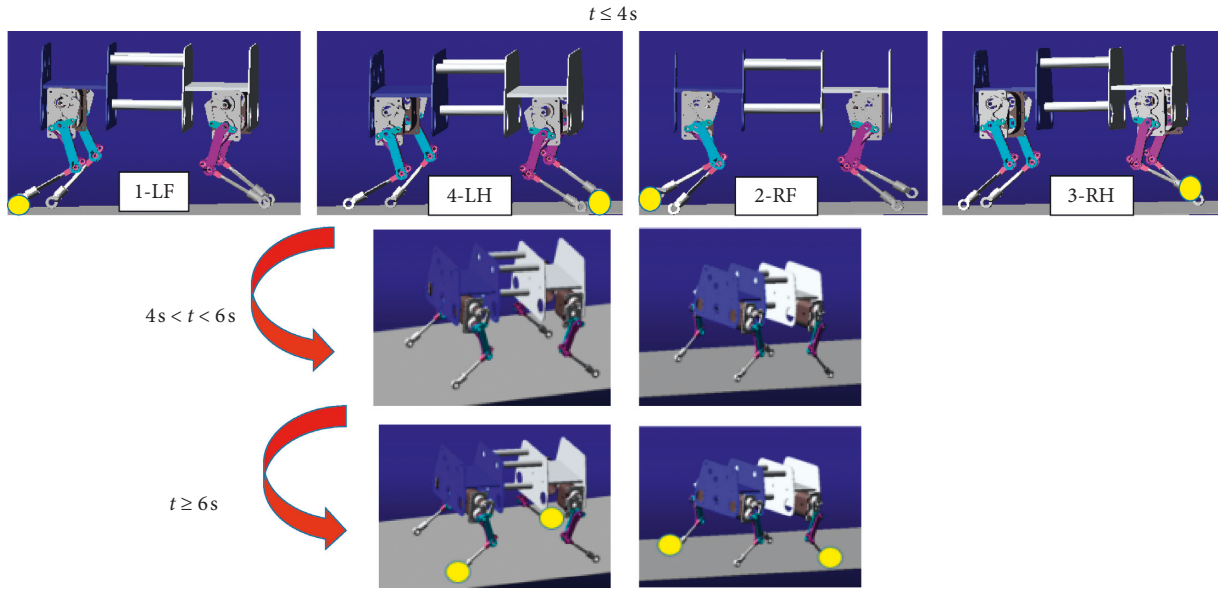


Figure 18: Walk-trot gait switching simulation.

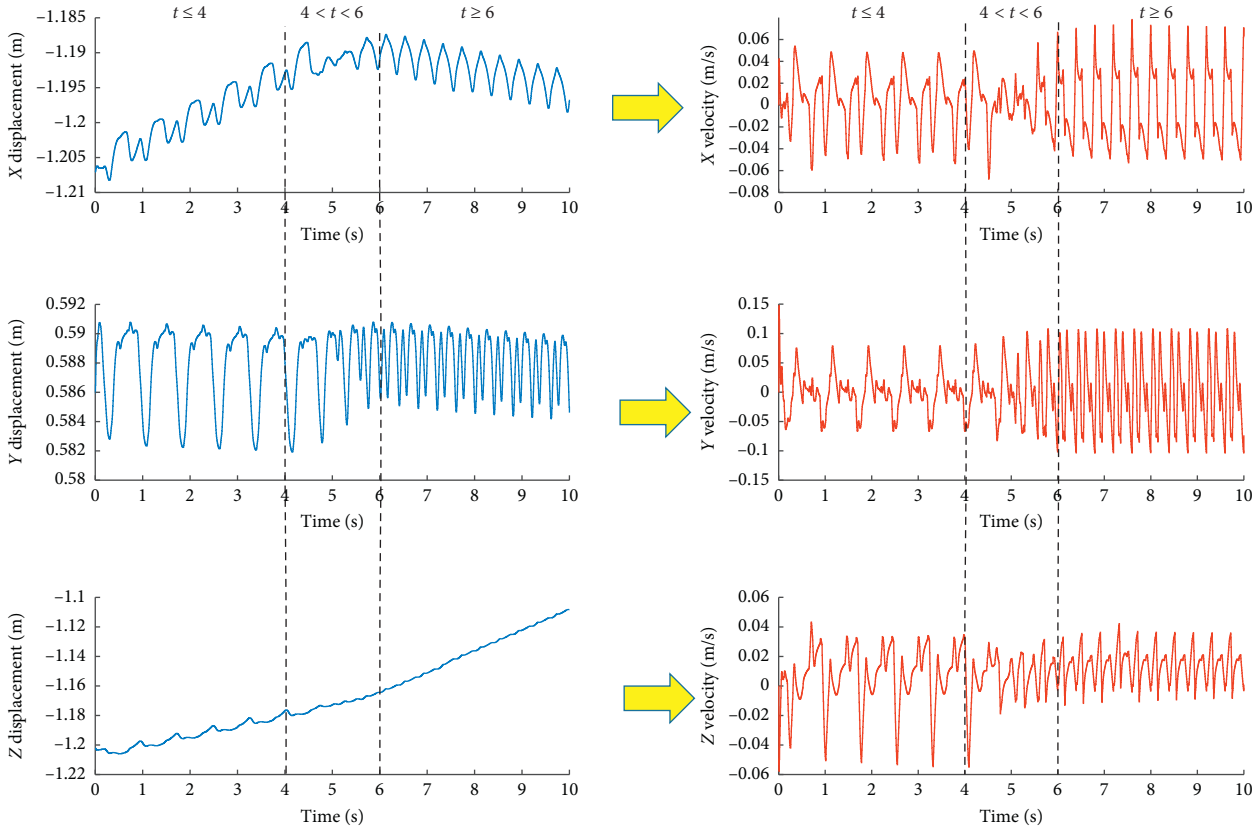


Figure 19: Displacement and speed in gait switching.

network lines. Compared with traditional Fieldbus technology, EtherCAT (Ethernet Control Automation) fieldbus system chooses Ethernet as its basic framework, which has the advantages of fast transmission speed, large data packet capacity, and long transmission distance. A complete EtherCAT system usually has one master station and a series of slave stations. The master station and slave station support almost all the topological structures such as bus, tree, and star. The CK3E series programmable multiaxis controller of PMAC has good openness and can write control program freely. It supports EtherCAT bus communication and has three types of 8-axis, 16-axis, and 32-axis. Because of the requirement of control performance, the 16-axis CK3E-1310 controller shown in Figure 20 is chosen to control the robot.

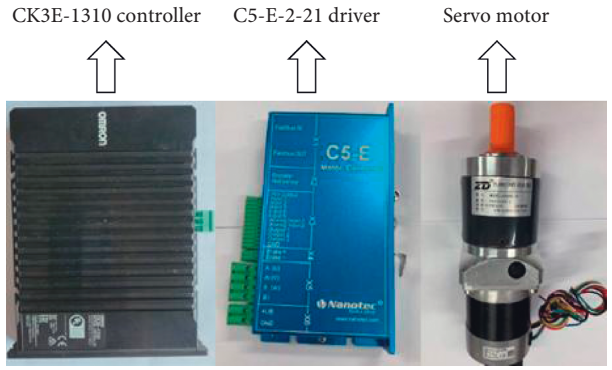


Figure 20: Control and drive system.

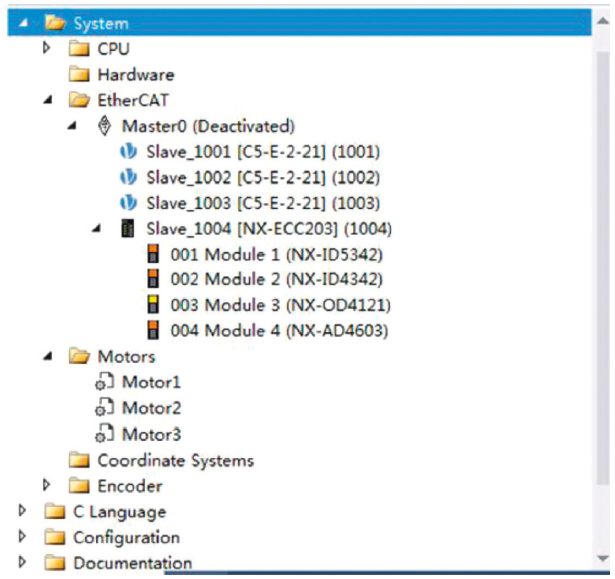


Figure 21: IDE programming interface.

CK3E Controller is programmed with POWERPMAC IDE Software, and its interface is shown in Figure 21. The CK3E controller is EtherCAT bus communication. Before writing all programs, it is necessary to build the EtherCAT network in the program. It includes scanning EtherCAT slave station, adding motor, establishing EtherCAT topology, and taking left front leg (LF) single leg structure as an example.

The single leg debugging lays the foundation for gait research and is also the precondition realizing the algorithm. By debugging the single leg motor, the movement law of the single leg can be obtained. In order to prevent the motor from blocking when the joint angle exceeds the limit position during the experiment, the debugging of the single leg structure should be completed before the whole machine is tested. The controller is connected with the PC terminal by the network line, and the debugging and downloading of the control program are completed. From the debugging results of Figure 22, it can be seen that the three motors can achieve specific motion in the range of rotation angle.

In order to verify the effectiveness of the proposed gait switching algorithm, an entity prototype model is built here as shown in Figure 23. The red circle represents the swing phase and the yellow circle represents the support phase. Because of the heavy body of the robot, the loss of DC power supply during walking is large. For the content of this paper, because only the gait experiment is involved, so the whole machine does not need to run on the ground, we built a frame to fix the fuselage. Write control program in IDE and debug communication between software and hardware. The controller generates the Hopf oscillator curve according to the driving requirement and applies the eight driving curves to eight joints of the robot to realize the specific gait of the robot. Figure 23(a) shows the initial state of a quadruped robot, in which the four legs are at the same height as the ground. When the time is 2 s, we can see from Figure 23(b) that the robot oscillates according to the phase difference of 0.25, and the oscillation law conforms to the static walking. When the robot runs to 8 s, we can see from Figure 23(c) that the diagonal leg swings back and forth with a phase difference of 0.5, thus realizing gait switching in a specific time range. Looking at the whole process, the quadruped robot can realize the smooth transformation from the walk gait to trot gait according to the given motion

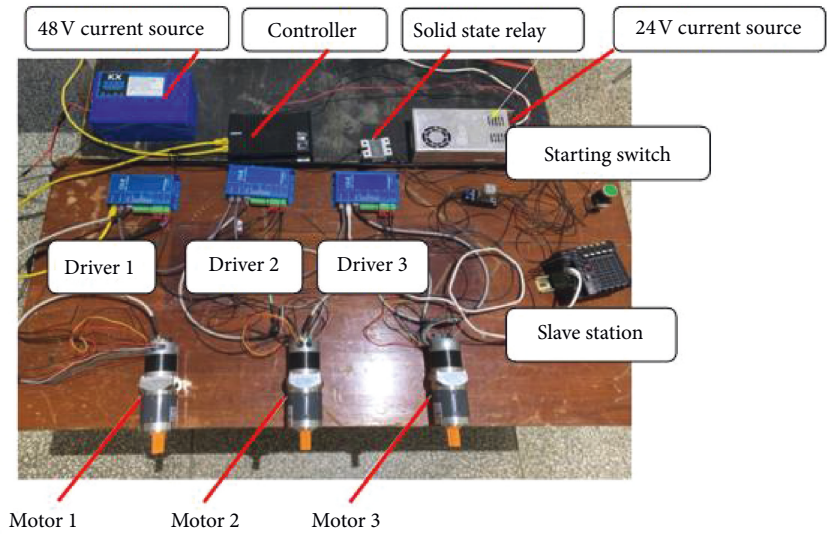


Figure 22: The single leg control debugging.

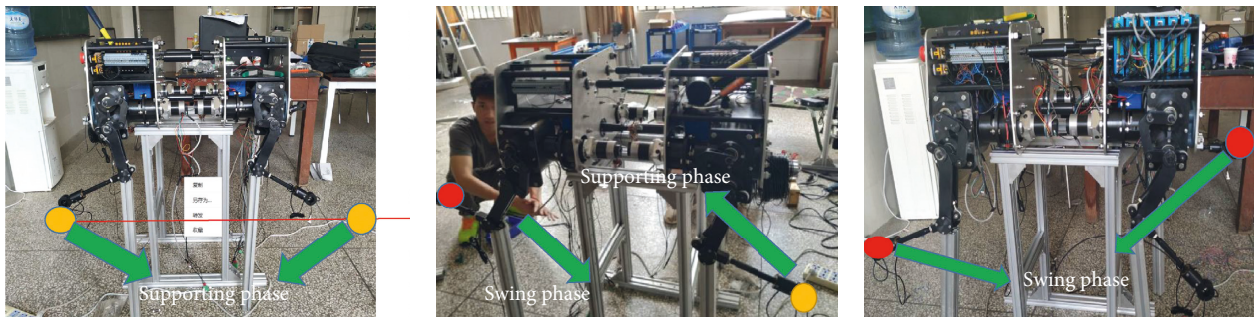


(a) (b) (c)

Figure 23: Gait switching process. (a) Initial position. (b) $T = 2$ s walk gait. (c) $T = 8$ s tort gait.

law, which proves the effectiveness of the proposed algorithm.

## 8. Conclusion

(1) In this paper, single leg structure with the anti-parallelogram is designed, which greatly improves the strength and stiffness of the leg and enhances the load capacity of the robot.

(2) The configuration of the whole robot and the structure of one leg are introduced, which lays a foundation for the research of the robot gait. The Hopf oscillator is introduced into parallelogram leg mechanism for the first time, which proves that the leg can be the gait realized by the Hopf oscillator.

(3) The CPG network topology is established, and the improved Hopf oscillator is used to control the robot joints. Simulink-ADAMS simulation platform is built to realize the walk and trot gait of the robot.

(4) In order to solve the problems of breakpoints, phase-locked, and stopping of the substitution gait matrix, a piecewise function is introduced to realize the smooth transition from the walk gait to the trot gait.

(5) Through the joint simulation, it can be found that the robot can operate according to the given driving law and the gait adjustment meets the requirements and has good stability.

(6) Experiments on one leg and the whole machine show that the robot can achieve a smooth transition from the walk gait to the trot gait, which proves the effectiveness of the proposed method.

## Data Availability

The data used to support the findings of this study are available from the corresponding author upon request.

## Conflicts of Interest

The authors declare that there are no conflicts of interest regarding the publication of this paper. The authors declare that the data and results generated by simulation and experiment are feasible.

## Acknowledgments

This research was financially supported by the National Key R&D Projects under Grant no. 2017YFC1702503 and the National Natural Science Foundation of China under Grant no. 51565021.

## References

[1] J. S. Gao, M. X. Li, B. J. Hou, and B. T. Wang, "Kinematics analysis on the series-parallel leg of a novel quadruped walking robot," *Optics and Precision Engineering*, vol. 23, no. 11, pp. 3147–3160, 2015.

[2] E. Mingcheng, H. Liu, X. L. Zhang, F. U. Chenglong, and M. A. Hongxu, "Compliant gait generation for a quadruped bionic robot walking on rough terrains," *Robot*, vol. 36, no. 5, pp. 584–591, 2014.

[3] X. Zhang, X. Qin, H. Feng, W. Zhao, J. Li, and X. Tan, "Design and experiment study on a quadruped robot single legwith composite rigid-flexible configuration for gallop gait," *Robot*, vol. 35, no. 5, pp. 582–588, 2013.

[4] M. Raibert, K. Blankespoor, G. Nelson, and R. Playter, "BigDog, the rough-terrain quadruped robot," in *Proceedings of the 17th IFAC World Congress*, pp. 10822–10825, Seoul, Korea, July 2008.

[5] M. Kalakrishnan, J. Buchli, P. Pastor, M. Mistry, and S. Schaal, "Learning, planning and control for quadruped locomotion over challenging terrain," *The International Journal of Robotics Research*, vol. 30, no. 2, pp. 236–258, 2011.

[6] H. Chai, J. Meng, X. W. Rong, and Y. Li, "Design and implementation of scalf, an advanced hydraulic quadruped robot," *Robot*, vol. 36, no. 4, pp. 385–391, 2014.

[7] K. Yoneda, F. Ito, Y. Ota, and S. Hirose, "Steep slope locomotion and manipulation mechanism with minimum degrees of freedom," in *Proceedings of the 1999 IEEE/RSJ International Conference on Intelligent Robots and Systems*, vol. 3, pp. 1896–1901, Kyongju, South Korea, October 1999.

[8] H. B. Wang, Z. Y. Qi, Z. W. Hu, and Z. Huang, "Application of parallel leg mechanisms in quadruped/biped reconfigurable walking robot," *Journal of Mechanical Engineering*, vol. 45, no. 8, pp. 24–30, 2009.

[9] C. Zhang and Y. Li, "A new walking robot based on 3-RPC parallel mechanism," *Journal of Mechanical Engineering*, vol. 47, no. 15, pp. 25–30, 2011.

[10] J. P. Chen, H. J. San, X. Wu, M. Chen, and W. He, "Structural design and characteristic analysis for a 4-degree-of-freedom parallel manipulator," *Advances in Mechanical Engineering*, vol. 11, no. 5, pp. 1–12, 2019.

[11] A. J. Ijspeert, "Central pattern generators for locomotion control in animals and robots: a review," *Neural Networks*, vol. 21, no. 4, pp. 642–653, 2008.

[12] S. Nicole and E. Pessa, "A network model with auto-oscillating output and dynamic connections," *Biological Cybernetics*, vol. 70, no. 3, pp. 275–280, 1994.

[13] J. Ingvast and W. Jan, "A passive load-sensitive revolute transmission," in *Proceedings of the International Conference on Climbling and Walking Robots*, pp. 2–5, Paris, France, September 2002.

[14] J. Li, C. Wu, and T. Ge, "Central pattern generator based gait control for planar quadruped robots," *Journal of Shanghai Jiaotong University (Science)*, vol. 19, no. 1, pp. 1–10, 2014.

[15] Q. Wu, C. Liu, J. Zhang, and Q. Chen, "Survey of locomotion control of legged robots inspired by biological concept," *Science in China Series F: Information Sciences*, vol. 52, no. 10, pp. 1715–1729, 2009.

[16] L. Righetti and A. J. Ijspeer, "Pattern generators with sensory feedback for the control of quadruped locomotion," in *Proceedings of the 2008 IEEE International Conference on Robotics and Automation*, pp. 819–824, Pasadena. CA, USA, May 2008.

[17] L. Righetti and J. Buchli, "From dynamic hebbian learning for oscillators to adaptive central pattern generators," in *Proceedings of the Third International Symposium on Adaptive Motion in Animals and Machines*, Ilmenau, Germany, September 2005.

[18] B. Van der Pol and J. Van der Mark, "LXXII. The heartbeat considered as a relaxation oscillation, and an electrical model of the heart," *The London, Edinburgh, and Dublin Philosophical Magazine and Journal of Science*, vol. 6, no. 38, pp. 763–775, 1928.

[19] J. S. Bay and H. Hemami, "Modeling of a neural pattern generator with coupled nonlinear oscillators," *IEEE Transactions on Biomedical Engineering*, vol. BME-34, no. 4, pp. 297–306, 1987.

[20] Y. Hu, J. Liang, and T. Wang, "Parameter synthesis of coupled nonlinear oscillators for CPG-based robotic locomotion," *IEEE Transactions on Industrial Electronics*, vol. 61, no. 11, pp. 6183–6191, 2014.

[21] X. Wu, L. Teng, W. Chen, G. Ren, Y. Jin, and G. Li, "CPGs with continuous adjustment of phase difference for locomotion control," *International Journal of Advanced Robotics Systems*, vol. 10, no. 6, pp. 1–13, 2013.

[22] C. P. Santos and V. Matos, *Gait Transition and Modulation & Environmental Adaptability for Quadruped Robot*, Tsinghua University, Beijing, China, 2004.

[23] H. D. Xu, S. Gan, J. Ren, B. Wang, and Y. Jin, "Gait CPG adjustment for a quadruped robot based on Hopf oscillator," *Journal of System Simulation*, vol. 29, no. 12, pp. 3092–3099, 2017.

[24] Z. K. Wang, C. R. Ji, Z. Yang et al., "A new kind of center pattern generator research based on Hopf oscillator," *Modular Machine Tool & Automatic Manufacturing Technique*, no. 5, pp. 5–9, 2009.

[25] L. P. WANG, *Research on Control and Gait Planning for a Hydraulic Quadruped Robot*, Beijing Institute of Technology, Beijing, China, 2014.

[26] Y. Zhao, *The Simulation of Quadruped Robot Based on MATLAB and ADAMS*, Shandong University, Shandong, China, 2014.

[27] F. Delcomyn, "Walking robots and the central and peripheral control of locomotion in insects," *Autonomous Robots*, vol. 7, no. 3, pp. 256–280, 1999.

[28] J. Nishii, "A learning model for oscillatory networks," *Neural Networks*, vol. 11, no. 2, pp. 249–257, 1998.

[29] S. Crossberg, C. Pribe, and M. A. Cohen, "Neural control of inter-limb oscillations: I. Human bimanual coordinated," *Biological Cybernetics*, vol. 77, no. 2, pp. 131–140, 1997.

[30] Q. S. luo and X. Luo, *Quadruped Bionic Robot Technology*, Bejing Institute of Technology Press, Beijing, China, 2015.

[31] C. C. Canavier, D. A. Baxter, J. W. Clark, and J. H. Byrne, "Control of multistability in ring circuits of oscillators," *Biological Cybernetics*, vol. 80, no. 2, pp. 87–102, 1999.